

APCI(+)-FT-ICR MS Analysis of Hydrocarbons Using Isooctane as Ionizing Reagent - A Comparison with HTGC-FID, GC×GC-MS and NMR

Lilian V. Tose,^a Samantha R. C. Silva,^b Eliane V. Barros,^a Lindamara M. Souza,^a Fernanda E. Pinto,^a Debora K. Palomino,^{b,c} Jair C. C. Freitas,^{b,c} Christopher J. Thompson,^d Boniek G. Vaz,^{a,e} Valdemar Lacerda Jr. *^a and Wanderson Romão*^{a,f}

^aLaboratório de Petroleômica e Forense, Departamento de Química, Universidade Federal do Espírito Santo, 29075-910 Vitória-ES, Brazil

^bLaboratório de Pesquisa e Desenvolvimento de Metodologias para Análise de Óleos (LabPetro), Departamento de Química, Universidade Federal do Espírito Santo, 29075-910 Vitória-ES, Brazil

^cLaboratório de Materiais Cerâmicos e Carbonosos, Departamento de Física, Universidade Federal do Espírito Santo, 29075-910 Vitória-ES, Brazil

^dBruker Daltonics, 40 Manning Road, 01821 Billerica-MA, USA

^eInstituto de Química, Universidade Federal de Goiás, 74001-970 Goiânia-GO, Brazil

^fInstituto Federal de Educação, Ciência e Tecnologia do Espírito Santo, 29106-010 Vila Velha-ES, Brazil

Hydrocarbons present in saturated fractions of crude oils can be assessed by atmospheric pressure chemical ionization (APCI) using small hydrocarbons as ionizing reagents in a Fourier transform ion cyclotron resonance mass spectrometer (FT-ICR MS). In this work, five paraffin standards of different average molar mass distributions (M_w) were easily ionized by APCI(+)-FT-ICR MS using isooctane as the reagent gas. Data of M_w , carbon number and double bond equivalent (DBE) distributions corresponding to linear and cyclic hydrocarbons (HCs) were compared to results obtained from analysis of high temperature gas chromatography with a flame ionization detector (HTGC-FID), comprehensive two-dimensional gas chromatography coupled to mass spectrometry (GC×GC-MS) and ¹H and ¹³C nuclear magnetic resonance (NMR) spectroscopy. APCI(+)-FT-ICR MS data showed good agreement with those of analytical techniques. Furthermore, the ability of APCI(+) to assess *n*-paraffin, even in blends with polyaromatic hydrocarbon molecules such as coronene ($M_w = 301$ Da) at concentrations from 2.5 to 25 $\mu\text{g mL}^{-1}$, was demonstrated. The typical MS paraffin profile (containing repeating mass units of 14 Da) was clearly confirmed, being totally suppressed when a concentration of 25 $\mu\text{g mL}^{-1}$ of coronene was used. This phenomenon was also evidenced in one of two saturated fractions produced using saturates, aromatics and polar (SAP) compound fractionation methodology.

Keywords: APCI(+)-FT-ICR MS, paraffin, HTGC, GC×GC-MS, NMR

Introduction

Fourier transform ion cyclotron resonance mass spectrometry (FT-ICR MS) provides unsurpassed mass resolution and accuracy, enabling the complex composition of petroleum,¹⁻³ its cuts,⁴ paraffin⁴⁻⁷ and asphaltene fractions to be analyzed on a molecular level.^{1,8-10} Accurate mass measurements define the unique elemental composition ($\text{C}_c\text{H}_h\text{N}_n\text{O}_o\text{S}_s$) and double bond equivalent (DBE),

facilitating material classification by heteroatom content and the degree of aromaticity.¹¹⁻¹³

Different methodologies have been proposed to improve the ionization of hydrocarbons (HCs) using mass spectrometry techniques. In 2004, Campbell *et al.*⁶ ionized saturated HCs using laser-induced acoustic desorption (LIAD) coupled to FT-ICR MS and assisted by chemical ionization with cyclopentadienyl cobalt radical cation (CpCo^{*+}). A unique ion was produced for each alkane from $\text{C}_{24}\text{H}_{50}$ to $\text{C}_{50}\text{H}_{102}$ composed of $[\text{R} + \text{CpCo} - 2\text{H}_2]^{*+}$, where R corresponds to the alkane. In 2012, Nyadong

*e-mail: vljuniorqui@gmail.com; wandersonromao@gmail.com

*et al.*⁷ presented an atmospheric pressure laser-induced acoustic desorption chemical ionization (AP/LIAD-CI) method with O₂ carrier/reagent gas as a powerful new approach for the analysis of saturated HCs mixtures. In the same year, Zhou *et al.*^{4,5} reported the development of a novel technique for the characterization of HCs, where linear alkanes were selectively oxidized to ketones by ruthenium ion catalyzed oxidation (RICO). The ketones were then reduced to alcohols by lithium aluminum hydride (LiAlH₄). The monohydric alcohols (O₁) were characterized using negative-ion electrospray ionization (ESI) coupled to FT-ICR MS for identification of isoparaffins, acyclic paraffins and cyclic paraffins.

In 2012, Lorente *et al.*¹⁴ reported a new analytical method for HCs identification using matrix-assisted laser desorption/ionization time-of-flight mass spectrometry (MALDI-TOF MS) with AgNO₃ and based on a combination of urea adduction and thin layer or paper chromatography. However, unidentified peaks were observed in the low-mass region ($m/z < 400$), being likely to have arisen from interactions between the silica on the plates and the AgNO₃ matrix. The method was also applied for the alkane fraction isolated by the standard urea adduction from crude oil samples.

Adapting the work of Gao *et al.*,¹⁵ Tose *et al.*¹⁶ noticed that linear, cyclic and branched paraffins have their ionization favored using HCs with carbon numbers (CNs) between C₅ and C₈ as reagents in the atmospheric pressure chemical ionization (APCI) source. Among them, the isooctane provided the best results when used as a solvent/reagent. The mechanism that best explains the ionization of linear HCs is hydride abstraction, i.e., the formation of [M – H]⁺ ions.¹⁵ This study is a continuation of the earlier work published by our group,¹⁶ where five paraffin standards of different average molar mass distribution (M_w) were ionized by APCI(+)-FT-ICR MS using isooctane as the reagent gas. Data of M_w, carbon number (CN) and DBE distributions corresponding to linear and cyclic HCs were compared to the results obtained by other analytical methods, such as high temperature gas chromatography with a flame ionization detector (HTGC-FID), comprehensive two-dimensional gas chromatography coupled to mass spectrometry (GC×GC-MS) and ¹H and ¹³C nuclear magnetic resonance (NMR) spectroscopy. Furthermore, the selectivity of the APCI(+) technique was also evaluated in the ionization of six commercial polyaromatic hydrocarbon (PAH) standards and mixtures between coronene (M_w = 301 Da) and a commercial paraffin sample. Finally, two saturated fractions produced from a saturate, aromatic and polar (SAP) compound fractionation methodology were analyzed by APCI(+)-FT-ICR MS and GC×GC-MS, with

a detailed comparison being carried out between the obtained results.

Experimental

Reagents and samples

Five paraffin standards, named standards P1-P5, containing carbon numbers ranging from C₅ to C₁₂₀ (analytical grades with purity higher than 99.5%) were used in this study. Standards P1 and P3 were supplied by Vetec Química Fina Ltda, Brazil; standard P2 was supplied by Sigma-Aldrich Chemicals, USA; standard P4 was the result of a commercial petrochemical process; and finally, standard P5 was a reference material used for GC-FID calibration (AC 655, USA). Isooctane (CAS No. 540-84-1) was supplied by Vetec Química Fina Ltda, Brazil (> 99.5%, UV/HPLC (high-performance liquid chromatography)), and used as an APCI reagent. Methanol (CAS No. 67-56-1), sodium trifluoroacetate (NaTFA, CAS No. 2923-18-4), L-arginine (CAS No. 74-79-3), and formic acid (HCOOH, CAS No. 64-18-6) were also purchased from Sigma-Aldrich Chemicals, USA (> 99%) and used for the FT-ICR MS calibration. All reagents were used as received without any further purification.

Six PAH standards were supplied by Sigma-Aldrich Chemicals, USA. They were named standards A1-A6 and they are: standard A1, 2,9-dipropylanthra[2,1,9-def:6,5,10d'e'f']diisoquinoline1,3,8,10(2*H*,9*H*)tetrone (≥ 97%, HPLC; CAS No. 59442-38-5); standard A2, EPA 8100 PAH additional components mix (97%, HPLC; product by Sigma-Aldrich reference number 44694-U); standard A3, benz[*a*]anthracene (98%, HPLC; CAS No. 56-55-3); standard A4, coronene (≥ 99%, HPLC; CAS No. 191-07-1); standard A5, *n,n'*-bis(3-pentyl)perylene-3,4,9,10-bis(dicarboximide) (≥ 99%, HPLC; CAS No. 110590-81-3); and standard A6, polynuclear aromatic hydrocarbons (97%, HPLC; CAS No. 110-82-7).

The SAP compound's fractions were separated by a preparative liquid chromatography column under medium-to-low vacuum for two crude oil samples, supplied by PETROBRAS, Brazil. The physicochemical properties of the two crude oils and the amounts of their respective SAP fractions are detailed in Table 1. For the fractionation, approximately 20 g of silica (230-400 mesh) was activated at 120 °C for 12 h and packed into a glass column of 1.6 cm diameter. To the top of the column, 200 mg of crude oil was added. Successive elution was performed with 200 mL of hexane (99% PA), 200 mL of dichloromethane:hexane 1:1 (% v/v) (99% PA for dichloromethane) and 200 mL of methanol (99.9%, HPLC), in order to separate the

Table 1. Physicochemical properties of the two crude oils used for saturates, aromatics and polar (SAP) fraction production. The confidence interval^a associated with the numerical data is shown in parentheses

Crude oil	API gravity ^b	Total acid number / (mg KOH g ⁻¹)	Kinematic viscosity at 40 °C / cSt	Pour point / °C	Total sulfur / wt. %	Saturates / wt. %	Aromatic / wt. %	Polar / wt. %
1	27.88 (0.15)	0.314 (0.024)	20.42 (0.25)	-12.0	0.3714 (0.001)	61.7	24.4	13.9
2	34.46 (0.55)	0.095 (0.009)	31.13 (0.23)	6.0	0.0575 (0.001)	75.5	15.0	9.6

^aConfidence interval (CI) values were calculated according to equation $CI = \text{standard deviation} \times [4.3/(3)^{1/2}]$, where 4.3 means the value of t (statistical parameter) for 2 degrees of freedom and 95% confidence level; ^bthe American Petroleum Institute gravity, or API gravity, is a measure inversely proportional to the relative density of the petroleum.

fractions of saturates, aromatics and polar compounds, respectively. The solvents were removed using a rotary vacuum evaporator to recover the SAP fractions. The results are described in Table 1; the percentages of saturated fractions produced from the two crude oil samples, named as fractions S_A and S_B , were equal to 62 and 76 wt.%, respectively.

Preparation of paraffins/PAH blends

To evaluate the efficiency of the APCI(+) technique to ionize HCs selectively, a paraffin sample (standard P4) was doped with coronene (standard A4) at concentrations of 2.5, 5, 15 and 25 $\mu\text{g mL}^{-1}$. Previously, the paraffin and coronene solutions were singly prepared at ca. 0.5 mg mL^{-1} in isooctane.

APCI(+)-FT-ICR MS

FT-ICR MS analysis was performed using a 9.4 T Q-FT-ICR MS hybrid (Solarix, Bruker Daltonics, Bremen, Germany) equipped with a commercial APCI source (Bruker Daltonics, Bremen, Germany) set to operate over m/z 200-2000. The paraffins and PAH commercial standards, saturated fractions, and paraffin/PAH mixtures were analyzed using positive ionization mode, APCI(+). The samples were diluted in isooctane to 0.5 mg mL^{-1} . The resulting solution was sonicated for 60 min at 40 °C and directly infused with a flow rate of 20 $\mu\text{L min}^{-1}$. The APCI(+) source conditions were as follows: nebulizer nitrogen gas temperature and pressure of 2.0 bar and 320 °C, capillary voltage of 4 kV, transfer capillary temperature of 180 °C, drying gas flow rate of 4 L min^{-1} , end plate offset of 500 V, skimmer of 35 V, collision voltage of -1.5 V, and corona discharge of 9 μA .

In the FT-ICR MS analyzer, a 0.02 s ion accumulation time was used in the hexapole followed by sample transport to the analyzer cell (ICR) through the multipole ion guide system (another hexapole). Each spectrum was acquired using 200 scans of time-domain transient signals in

4 megapoint time-domain data sets. The front and back trapping voltages in the ICR cell were +0.80 and +0.85 V, respectively, for positive ionization mode. All mass spectra were externally calibrated using L-arginine (200-2000 m/z), then internally recalibrated using the most abundant homologous alkylated compounds in each sample.¹⁷⁻²² The tandem mass spectrometry (MS²) experiments were performed on a quadrupole coupled to an FT-ICR mass spectrometer, Q-FT-ICR MS. APCI(+)-MS/MS experiments were performed using collision energies of 15-30% for the ions of m/z 561, 589, 603, 645, 673, and 701, and 0-30% for the two PAH commercial standards (ions of m/z 229 and 301).²³

The resolving power ($m/\Delta m_{50\%}$ from 420,000 to 530,000, where m corresponds to m/z 400 and $\Delta m_{50\%}$ is the full peak width at half-maximum peak height) and mass accuracy lower than 1-3 ppm provided the unambiguous molecular formula assignments for all singly charged molecular ions. The mass spectra were acquired and then processed with a custom algorithm specifically developed for petroleum data using the Composer software package.²⁴ The MS data were processed and the elemental compositions of the molecules were determined by measuring the m/z values. Class, DBE distributions and CN *versus* DBE plots were constructed to allow the interpretation of the results.^{1,3,4,13,17,25} For the CN *versus* DBE and DBE *versus* intensity plots, DBE was the number of rings added and the number of double bonds in each molecular structure. The unsaturation level of each compound can be deduced directly from its DBE value, according to equation 1:

$$DBE = C - \frac{H}{2} + \frac{N}{2} + 1 \quad (1)$$

where C, H and N are the numbers of carbon, hydrogen and nitrogen atoms, respectively, in the molecular formula.

High-temperature gas chromatography (HTGC)

The HTGC analyses of paraffin standards and saturate fractions were performed using Agilent 6890 N Network

GC System customized by Analytical Control (AC, Netherlands) with a flame ionization detector (FID). Paraffin samples were diluted in CS₂ at 2 wt.%, and 1 µL of sample was injected into the HT750 capillary column (5 m × 0.53 mm × 0.1 µm, from AC) using an auto-injector. The HTGC was calibrated using a standard mixture containing carbon numbers from C₅ to C₁₂₀, according to the ASTM D7169-05²⁶ standard. The analyses were performed under a helium flow rate of 15 mL min⁻¹ and a temperature program of -20 to 430 °C at 10 °C min⁻¹.

The initial temperature of the injection port was 50 °C, which was increased to 430 °C at a rate of 15 °C min⁻¹, and then kept constant for 26 min. The detector was kept at 430 °C. The data acquisition frequency was 10 Hz. The HTGC data were analyzed using GC ChemStation Rev. B.03.01-1.1 SR-[317] software, and version 8.4.0.0.

¹H and ¹³C NMR spectroscopy

¹H and ¹³C NMR spectra of the five paraffin standards were recorded on a Varian VNMRs 400 spectrometer, operating at 9.4 T and using a 5 mm broadband ¹H/X/D probe. The experiments were performed at 25 °C, using 20 mg of paraffin diluted in 0.6 mL of deuterated chloroform. Tetramethylsilane (TMS) was used as an internal standard for setting the chemical shift scale. A spectral width of 6410.3 Hz was used, with a relaxation delay of 1.5 s, and 512 transients were accumulated for each spectrum. The relaxation agent Cr(Acac)₃ diluted in deuterated chloroform at 50 mM was also employed. For the ¹³C NMR, the same solution used in the ¹H NMR experiments was employed, with a spectral width of 25510.2 Hz, a relaxation delay of 15 s and 20,000 scans, with a pulse flip angle of 90° (9.5 ms). The decoupler mode was switched off during the pulse and the standby time was switched on during data acquisition to avoid nuclear Overhauser Increase Effect (NOE). The spectra obtained for the paraffin standards were integrated from 9.0 to 6.0 ppm (for the aromatic hydrogen region) and from 4.0 to 0.0 ppm (for the aliphatic hydrogen region). This procedure was analogous to the method described by Oliveira *et al.*²⁷

Two-dimensional gas chromatography (GC×GC-MS)

The paraffin standards (P1-P3) and two saturated fractions from petroleum (denominated by fractions S_A and S_B) (all at 500 mg L⁻¹) were analyzed by GC×GC-MS (Shimadzu QP2010 Ultra system, USA) with a ZX1-GC × GC modulator (Zoex, Houston, TX, USA). The chromatographic separation was performed by two columns,

in which the first column was based on DB-5, 5% phenyl and 95% methylpolysiloxane (30 m × 0.25 mm i.d. × 0.25 µm film thickness, J&W Scientific, Agilent Technologies, USA) and the second column was DB-17, 50% phenyl and 50% methyl-polysiloxane (1.8 m × 0.10 mm × 0.10 µm, J&W Scientific, Agilent Technologies, USA). The oven temperature programming started at 140 °C for 5 min, then a ramp of 2 °C min⁻¹ to 310 °C, and finally 310 °C for 10 min, for a total analysis time of 100 min. The injector temperature/interface and ion source were maintained at 300 °C. The analyses were performed using the splitless mode, and helium gas (5.0) was used as a constant carrier gas at a flow of 1.5 mL min⁻¹. The mass range was examined from 50 to 600 Da, with a modulation period of 8 s. GC Image software (ZOEX Corporation, Houston, Texas, USA) was used for the identification of compounds.

Results and Discussion

Paraffin standards

Figures 1a-1e show the APCI(+)-FT-ICR mass spectra obtained for the five paraffin standards (standards P1-P5). Standards P1, P2 and P3 had an *m/z* distribution ranging from 200 to 650, with average molecular weights (*M_w*) centered at *m/z* 431, 444 and 572, respectively. These distributions corresponded to carbon numbers (CNs) ranging from C₁₆ to C₄₈. On the other hand, wider distributions of HCs (*m/z* 200-800 and *m/z* 200-1200) were observed for standards P4 and P5, being indicative of the existence of high molecular weight HCs with CNs ranging from C₁₆ to C₅₈ and C₃₀ to C₇₆, respectively. These species were ionized via loss of a hydride (H), thus forming [M - H]⁺ cations.

The inset around the *m/z* 323 region in Figure 1 displays a major signal of *m/z* 323.3673 corresponding to the [C₂₃H₄₈ - H]⁺ cation with DBE = 0. Low abundance heteroatom HC species corresponding to nitrogenated and oxygenated compounds were also detected as [C₂₂H₄₄O - H]⁺ and [C₁₉H₃₆N₂O₂ - H]⁺ cations, with *m/z* 323.3309 and 323.2693 and DBEs of 1 and 2, respectively. These compounds originated from ion molecule reactions between sheath gas (N₂), APCI reagent (isooctane) and O₂ (from ambient atmosphere) with HC compounds in the presence of the corona discharge.^{7,16}

Generally, APCI(+) analysis demonstrated to be efficient in the ionizing of HCs. Therefore, APCI(+) is a desirable technique, since the identification of saturated and/or unsaturated HCs (specifically *n*-paraffins, isoparaffins and cycloparaffins) are the major contributors to understanding the process of paraffin deposition that occurs during the production, transportation and oil refining.¹⁶

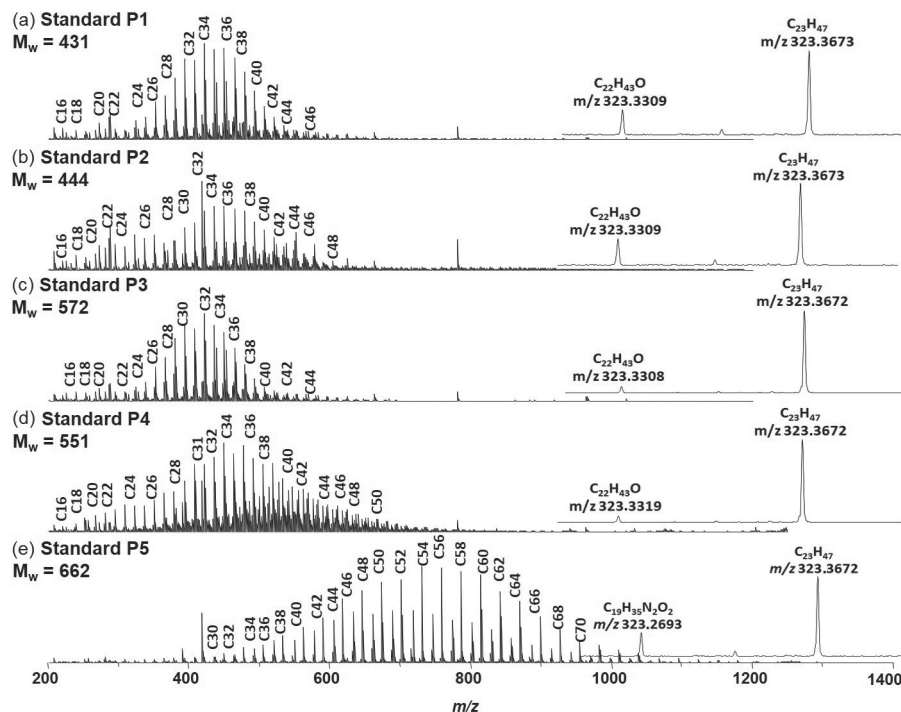


Figure 1. APCI(+)-FT-ICR mass spectra for paraffins standard P1-P5 prepared at 0.5 mg mL^{-1} in isoctane.

Chromatograms from the HTGC analysis of standards P1-P5 are shown in Figures S1a-S1e (Supplementary Information (SI) section), and were done in order to establish a comparison with the APCI(+)-FT-ICR MS technique. HCs were identified on the basis of retention times of known *n*-paraffins, where their CNs ranged from C_{10} to C_{100} . Figure S1 (SI section) shows that the CNs of *n*-paraffins present in standards P1-P3 varied from C_{15} to C_{39} , whereas for standards P4 and P5 varied from C_{18} - C_{46} and C_8 - C_{100} , respectively. However, the HTGC technique identifies only saturated HCs, whereas branched and cyclic HCs are not resolved.^{6,7} On the other hand, APCI(+)-FT-ICR MS is able to distinguish the chemical composition of paraffins between saturate/branch and cyclic HCs.¹⁶

In order to facilitate the visualization of APCI(+)-FT-ICR MS data, diagrams of classes were constructed, and their abundances were in the following order: $\text{HC}[\text{H}] > \text{N}[\text{H}] > \text{O}[\text{H}] > \text{NO}[\text{H}] \text{ ca. } \text{NO}_2[\text{H}] > \text{O}_2[\text{H}] > \text{other}$ (the transfer of protons or abstraction of hydrides is represented by [H] associated with the class who it refers) (Figure 2a). APCI(+) assisted by isoctane reagent proved to be effective for the selective ionization of HCs, where these species were dominant in standards P3 and P4 (Figure 2a). All paraffins standards showed heteroatomic compounds, where a higher abundance of these compound classes was found in standards P1 and P5 (Figure 2a).

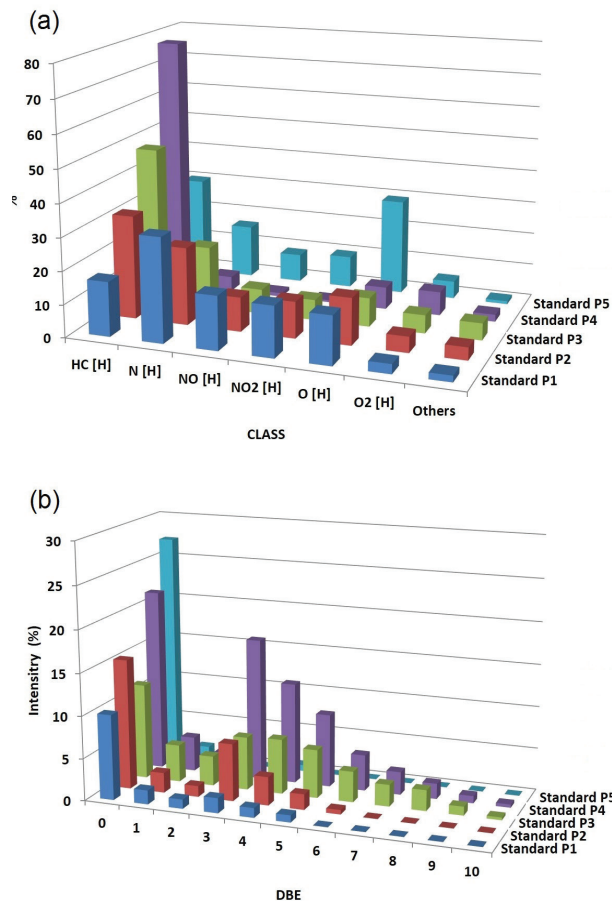


Figure 2. Class diagrams (a) and DBE distribution for HC class (b) for paraffins standard P1-P5 obtained from APCI(+)-FT-ICR MS data.

Plots of DBE *versus* intensity were also constructed (Figure 2b), and a lower DBE distribution was observed for standards P1, P2 and P5, whereas for standards P3 and P4, the DBE values varied from 0 to 9. DBE values higher than 1 are indicative of the presence of polycyclic paraffins (cycloalkanes and naphthenes) as well as of PAH species. Despite the existence of HCs with DBE \neq 0, the relative abundance of saturate HCs (i.e., DBE = 0) were always highest (Figure 2b).

The chemical profile of CN distribution among the paraffin samples is shown in Figures S2a-S2e (SI section) from the construction of DBE \times CN plots. Differently from other samples, a wider and richer CN distribution was only observed for standard P5, which had aliphatic HCs (DBE = 0) containing CNs ranging from C₂₀ to C₇₈, with the maximum distribution centered at C₄₇. This result was in good agreement with HTGC data, which showed a CN distribution ranging from C₈ to C₈₆ with a maximum centered at C₄₆ (Figure S1e, SI section). For standards P3 and P4, the detection of polycyclic HCs was more evident (Figures S2c-S2d, SI section), where two sets of distributions are visualized: aliphatic HCs (DBE = 0 with CNs of C₁₅-C₆₀) and cyclic and polycyclic HCs (DBE \geq 2 and DBE \leq 7 containing CNs of C₂₀-C₅₈). HTGC data confirmed the existence of *n*-paraffins containing CNs in the ranges of C₂₀-C₃₉ and C₂₀-C₄₆ for standards P3 and P4, respectively (Figures S1c-S1d, SI section). Low intensity and unresolved peaks due to unidentified compounds were observed in HTGC chromatograms obtained for standards P1-P4, as well as a shift of baseline (Figures S1a-S1d, SI section). This behavior is indicative of the existence of polycyclic HCs, which were confirmed by the results obtained by APCI(+) technique.

To confirm the structure and connectivity of saturated and cyclic HCs in the paraffin standards, and also to discard the existence of PAHs for the set of molecules of HC[H] class with DBE \geq 4, collision induced dissociation (CID) experiments were performed for HCs ions having different DBEs (from 0 to 8) in standard P4. Figures 3a-3f show the APCI(+)-MS/MS results for the ions of *m/z* 701.7896 ([C₅₀H₁₀₂ - H]⁺, error = 0.28 ppm and DBE = 0, Figure 3a), *m/z* 645.72343 ([C₄₆H₉₄ - H]⁺, error = 5.81 ppm and DBE = 0, Figure 3b), *m/z* 561.5378 ([C₄₁H₇₀ - H]⁺, error = 2.85 ppm and DBE = 2, Figure 3c), *m/z* 673.6625 ([C₄₉H₈₆ - H]⁺, error = 3.12 ppm and DBE = 3, Figure 3d), *m/z* 589.5706 ([C₄₃H₇₄ - H]⁺, error = 0.01 ppm and DBE = 8, Figure 3e) and *m/z* 603.5803 ([C₄₄H₇₆ - H]⁺, error = 3.63 ppm and DBE = 8, Figure 3f). All ions showed similar fragmentation profiles with subsequent losses of 28 Da, referring to the ethene group (CH₂=CH₂). This result is similar to that obtained by Wu *et al.*²⁸ who analyzed

vacuum gas oil saturates by DESI-Orbitrap. Generally, this behavior provides evidence that PAHs are not a significant portion of the paraffins standards.^{22,23}

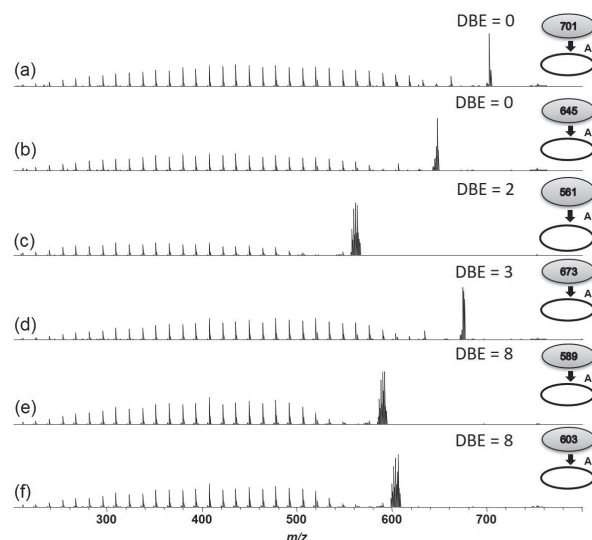


Figure 3. APCI(+)-MS/MS for ions at (a) *m/z* 701 (DBE = 0), (b) *m/z* 645 (DBE = 0), (c) *m/z* 561 (DBE = 2), (d) *m/z* 673 (DBE = 3), (e) *m/z* 589 (DBE = 8) and (f) *m/z* 603 (DBE = 8), corresponding to standard P4.

From the APCI(+)-MS/MS spectra, DBE *versus* CN plots were constructed for ions of *m/z* 701, 645, 561, 673, 589, and 603 (standard P4, Figures 4a-4f), corresponding to the HC[H] class. For the ions of DBE = 0 (*m/z* 701 and 645), the produced fragments showed a continuous distribution of CNs ranging from C₁₈ to C₄₃ with DBE = 0 for *n*-paraffin molecules (Figures 4a-4b). However, for cyclic paraffins (DBE = 8, Figures 4e-4f), abundant and minority groups of fragments were observed at DBE = 2 and 5-8 (cyclic HCs fragments) as well as the production of a non-continuous distribution of fragments at DBE = 0 containing CNs between C₁₆ and C₄₀. Hence, it is possible to note that the fragmentation profiles of saturate and cyclic HCs are similar to one another, but completely different from PAH molecules.²⁸

With the aims of quantitatively evaluating the possible presence of PAHs in the paraffin standards and better understanding their structural features, ¹H and ¹³C NMR spectra were recorded, as shown in Figures S3 and S4 (SI section). Due to the higher chemical shift range involved, ¹³C NMR spectra usually allow a more detailed structural study of paraffins, despite the inferior sensitivity of the ¹³C NMR technique as compared to ¹H NMR.²⁹⁻³²

Figure S3 (SI section) shows the ¹H NMR spectra of paraffin standard samples, where, essentially, the chemical shifts were assigned to ¹H nuclei in methylene groups (CH₂), labelled as H_β (1.0-1.8 ppm), or in methyl groups (CH₃), labelled as H_α (0.4-1.0 ppm). It is evident that, in all

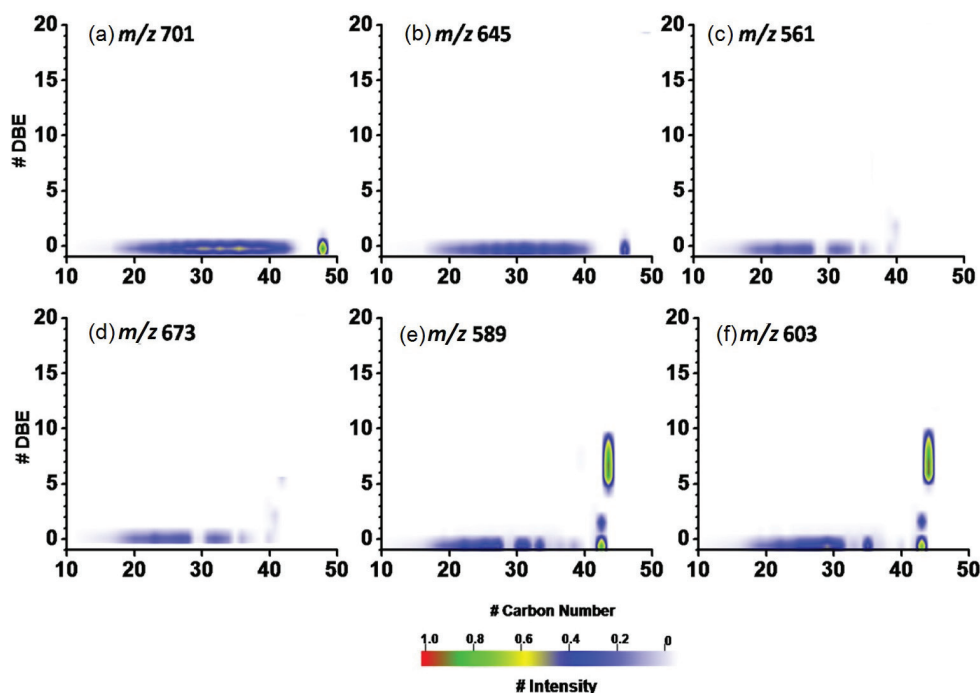


Figure 4. DBE versus CN plots for the HC[H] class from APCI(+)-MS/MS data of ions of m/z 701 (a), 645 (b), 561 (c), 673 (d), 589 (e) and 603 (f).

samples, the H_{β} signal (with relative intensity of ca. 90%) was much more intense than the H_{α} signal (relative intensity of ca. 10%) (Table 2). This behavior is typical of *n*- and isoparaffins with long chains,²⁹⁻³¹ since methyl groups (H_{α}) are present at the paraffin chain end or at the branching points, while methylene groups (H_{β}) compose the inner structure of the chains in *n*-paraffins and cyclic paraffins. Alcazar-Vara *et al.*³³ used ^1H and ^{13}C NMR to describe the mechanisms involved in the asphaltene-paraffin interaction and its effect on paraffin precipitation, and it was possible to determine the index of alkyl substitution in aromatic cores as well as the average length of the alkyl chains.³³

Analyzing the H_{ar} (total aromatic hydrogens) content, which was obtained by calculating the relative spectral intensity in the region of the ^1H NMR spectra that corresponded to aromatic hydrogens (δ 6.5-9.5 ppm), it was possible to disregard the presence of PAHs in the paraffin standard samples. Note that H_{ar} contents were

0.0 mol%, whereas H_{alk} (total aliphatic hydrogens) contents were 100.0 ± 0.0 mol% in almost all cases. Also, a good agreement was observed between the APCI(+)-MS and ^1H NMR data, with the H_{β} contents being directly associated with the average M_w values, which increased in the following order: standard P1 ($M_w = 431$ Da) < standard P2 ($M_w = 444$ Da) < standard P4 ($M_w = 551$ Da) < standard P3 ($M_w = 571$ Da) < standard P5 ($M_w = 662$ Da). It is clear from the data given in Table 2 that the H_{β} contents of the different samples grew exactly in the same order. However, when analyzing the standard deviation of the samples, standards P2, P3, and P4 presented close values of H_{β} . In fact, the H_{β}/H_{α} ratio in ^1H NMR spectra has also shown to be a good indicator of the average chain length of *n*-paraffins.³⁰⁻³² High deviation observed for the H_{α} and H_{β} values in standard P5 can be explained due to replicates analysis performed on different days. Besides, this sample displays a lower solubility in organic solvents at environmental temperature

Table 2. Classification of hydrogen types present in the paraffin standards according to ^1H NMR data. The confidence interval associated with the numerical data is shown in parentheses. The analyses were performed in triplicates

Molecular parameter	Relative quantity / mol%				
	Standard P1	Standard P2	Standard P3	Standard P4	Standard P5
$H_{\text{alk}}^{\text{a}}$	100.0 (0.0)	100.0 (0.0)	100.0 (0.0)	100.0 (0.0)	100.0 (0.1)
H_{ar}^{b}	0.0 (0.0)	0.0 (0.0)	0.0 (0.0)	0.0 (0.0)	0.0 (0.1)
H_{α}^{c}	11.4 (2.9)	10.8 (2.9)	9.9 (0.8)	10.2 (1.2)	5.2 (11.1)
H_{β}^{d}	88.6 (2.9)	89.2 (2.8)	90.1 (0.8)	89.8 (1.2)	94.8 (11.0)

^aTotal aliphatic hydrogens; ^btotal aromatic hydrogens; ^cmethyl hydrogen atoms; ^dmethylene hydrogen atoms.

due to its high M_w value, thus interfering, in precision of instrument.

Figure S4 (SI section) shows the ^{13}C NMR spectra obtained for the paraffin standards. Similar to what was reported by Cookson and Smith,³⁰ and assuming a paraffin molecule modelled as a linear chain, five chemical shifts (δ 14.3, 23.0, 32.2, 29.7, and 30.0 ppm) were assigned to chains of the type $(\alpha\text{CH}_3)_2(\beta\text{CH}_2)_2(\gamma\text{CH}_2)_2(\delta\text{CH}_2)_2(\epsilon\text{CH}_2)$, with the mentioned δ values corresponding to αCH_3 , βCH_2 , γCH_2 , δCH_2 , and ϵCH_2 groups, respectively, whose intensities are given in Table 3. Also, the (βCH_2) , (γCH_2) and (δCH_2) groups can indicate the presence of cycloparaffinic structures.^{30,32,34,35} Similar to the previously discussed ^1H NMR results, the relative intensity due to ϵCH_2 groups (δ 30.0 ppm) is directly related to the average chain length^{30,32} and, thus, to the M_w values, which increased in the following order: standard P1 < standard P2 < standard P4 < standard P3 < standard P5. This behavior is similar to the observed H_β contents. On the other hand, the abundance of cycloparaffinic structures (visualized from DBE *versus* CN plots, Figure S2, SI section) was correlated with the decrease of αCH_3 , γCH_2 and δCH_2 contents. Therefore, the cyclization degree decreased in the following order: standard P1 < standard P2 < standard P3 \approx standard P4 < standard P5 (Table 3). As observed in the content of H_β standards P3 and P4 presented close values of relative quantity (mol%), while standard P5 presented a value approximately 10% higher.

GC \times GC-MS elucidated the molecular composition of HCs, classifying them as linear, branched, cyclic and PAHs. Herein, three paraffin standard samples were investigated (standards P1-P3), and the two-dimensional chromatograms results are shown in Figures 5a-5c. A similar chemical profile containing CNs of linear-HCs ranging from C_{19} to C_{36} was identified for all samples. Other HC groups were also detected, such as alkyl-cyclopentane (A), alkyl-cyclohexene (B), alkyl-methyl-cyclohexene (C) and branched HCs (D), which were mostly present in standards P2 and P3 (Figures 5b-5c).

Despite the similarity in chemical composition among the three standards, paraffin standard P1 had a greater abundance of linear and branched HCs, while the other two samples had a greater abundance of cyclic paraffins, with DBEs of 1 (alkyl-cyclopentane) and 2 (alkyl-cyclohexene and alkyl-methyl-cyclohexene). Deursen *et al.*³⁵ also employed a two-dimensional system coupled to TOF-MS for analysis of crude oil samples, where it was possible to distinguish between saturated and cyclic HCs compounds. GC \times GC/q-MS results were in partial agreement with the DBE *versus* CN plots, as shown for the HC[H] class from APCI(+)-FT-ICR MS data (Figure S2, SI section). Cyclic paraffins were mostly present, although containing a higher amplitude of DBE values (DBE from 1 to 7) with the maximum distribution centered at DBE = 3 and CN of C_{30} (for standard P2) and C_{36} (for standard P3, see Figures S2b-S2c, SI section). This difference is due to the fact that APCI(+) renders the ionization of a wider distribution of HCs when compared with the GC \times GC/q-MS technique. Finally, the presence of PAHs was also not detected in any of three samples in the GC \times GC/q-MS data, being similar to NMR and APCI(+)-FT-ICR MS results.³⁵⁻³⁸

PAH standards and PAH/paraffin blends

The ability of APCI(+) to ionize PAH standards was also evaluated. Six commercial standards were investigated, and their APCI(+)-FT-ICR mass spectra are displayed in Figures S5a-S5f (SI section). In general, the PAHs were ionized via proton transfer ($[\text{M} + \text{H}]^+$), and the values of theoretical mass, experimental mass, mass error (ppm), molecular formula and DBE are shown in Table 4. APCI(+) caused the ionization of a single molecule for the standards A1, A3, A4 and A5, corresponding to $[\text{C}_{30}\text{H}_{22}\text{N}_2\text{O}_4 + \text{H}]^+$, $[\text{C}_{18}\text{H}_{12} + \text{H}]^+$, $[\text{C}_{24}\text{H}_{12} + \text{H}]^+$ and $[\text{C}_{34}\text{H}_{30}\text{N}_2\text{O}_4 + \text{H}]^+$ species, respectively. For standard A1, signals with $m/z < 300$ corresponded to fragmentation products (Figure S5a, SI section). In all cases, an accurate mass lower than 3 ppm was reported as well as DBE values between 9 and 21. For

Table 3. Classification of carbon types present in the paraffin standards according to ^{13}C NMR data. The confidence interval associated with the numerical data is shown in parentheses. The analyses were performed in triplicates

Molecular parameter	Relative quantity / mol%				
	Standard P1	Standard P2	Standard P3	Standard P4	Standard P5
αCH_3	7.4 (1.0)	6.6 (2.5)	6.2 (2.5)	5.8 (1.8)	4.1 (0.9)
βCH_2	7.8 (0.6)	6.9 (2.2)	6.6 (2.6)	6.2 (2.1)	3.1 (1.1)
γCH_2	7.7 (0.3)	6.8 (1.6)	6.4 (1.6)	5.8 (0.7)	2.8 (0.8)
δCH_2	7.9 (1.2)	7.0 (0.5)	6.6 (0.1)	6.3 (0.7)	2.4 (4.3)
ϵCH_2	69.2 (0.7)	72.7 (6.8)	74.2 (6.8)	75.9 (5.2)	87.3 (6.1)

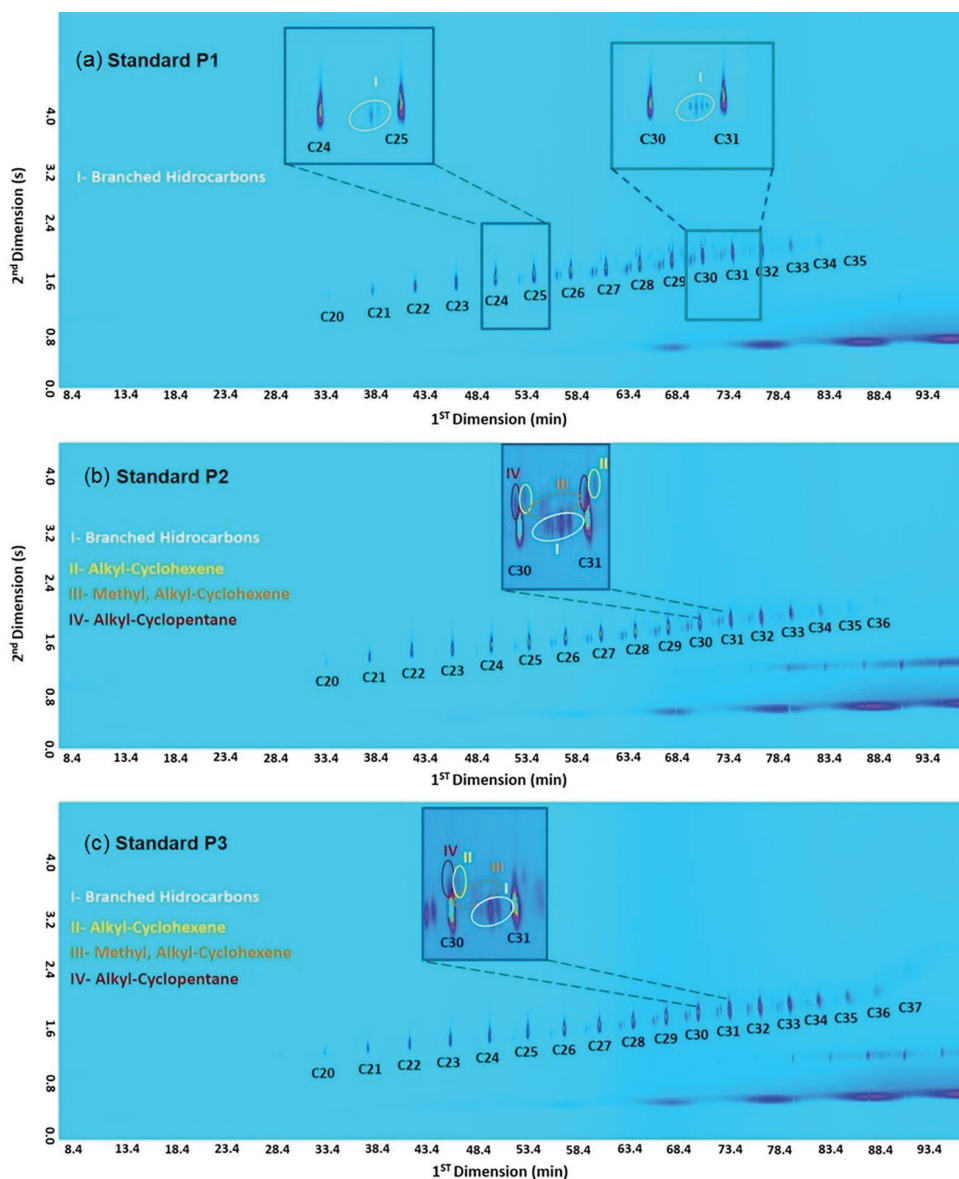


Figure 5. GCxGC/q-MS chromatograms of three paraffin standards (samples P1-P3).

Table 4. Values of theoretical mass, experimental mass, mass error, molecular formula and DBE for the PAH standards analyzed by APCI(+)-FT-ICR MS

^a PAH standard	Measured m/z	Theoretical m/z	Error / ppm	Molecular formula	^b DBE
A1	475.16664	475.16523	2.67	$[C_{30}H_{22}N_2O_4 + H]^+$	21
A2	253.10064	253.10118	2.13	$[C_{20}H_{12} + H]^+$	15
	269.13244	269.13248	0.15	$[C_{21}H_{16} + H]^+$	14
	303.11635	303.11683	1.58	$[C_{24}H_{14} + H]^+$	18
A3	229.10077	229.10118	1.79	$[C_{18}H_{12} + H]^+$	13
A4	301.10045	301.10118	2.42	$[C_{24}H_{12} + H]^+$	19
A5	531.22862	531.22783	1.49	$[C_{34}H_{30}N_2O_4 + H]^+$	21
A6	229.10077	229.10118	1.79	$[C_{18}H_{12} + H]^+$	13
	253.10072	253.10118	2.10	$[C_{20}H_{12} + H]^+$	15
	309.16345	309.16378	1.07	$[C_{24}H_{20} + H]^+$	15

^aPAH: polyaromatic hydrocarbon; ^bDBE: double bond equivalent.

the standards A2 and A6, a mixture of PAHs molecules was detected. They were $[C_{20}H_{12} + H]^+$, $[C_{21}H_{16} + H]^+$, and $[C_{24}H_{14} + H]^+$ ions (Figure S5b, SI section) and $[C_{18}H_{12} + H]^+$, $[C_{20}H_{12} + H]^+$, and $[C_{24}H_{20} + H]^+$ ions (Figure S5f, SI section, and Table 4), respectively.

In order to provide a comparison of the fragmentation standards of PAHs with acyclic and cyclic paraffins, CID experiments were performed for two PAH molecules: coronene (standard A4, m/z 301.10045, $[C_{24}H_{12} + H]^+$) and benzoanthracene (standard A3, m/z 229.10077, $[C_{18}H_{12} + H]^+$). APCI(+)MS/MS spectra are shown in Figures S6a-S6b (SI section), where, in both cases, mainly the elimination of a hydrogen radical, 1 Da ($\bullet H$), was observed. This fragmentation profile remained constant independent of the applied collision energy (ranging from 0 to 30 eV). The increase in the collision energy caused only the reduction of the total ion count as well as the reduction of intensity of the parent ions, m/z 301 and 229.

The efficiency of ionization of APCI(+) using isooctane as ionizing reagent was tested for mixtures between a PAH standard and *n*-paraffins. To verify this behavior, the paraffin standard P4 was doped with coronene ($[M + H]^+$ cation of m/z 301) at concentrations from 2.5 to 25 $\mu\text{g mL}^{-1}$. Figure 6 shows the APCI(+) FT-ICR mass spectra obtained for the coronene/paraffin blends, where it is clearly evident that the paraffin-related Gaussian profiles were progressively suppressed with the increase in the coronene concentration (m/z 301). A maximum suppression was observed at 25 $\mu\text{g mL}^{-1}$ of coronene (Figure 6a). This behavior could also be observed from the DBE distribution histograms versus intensity (Figure 6b), where at low coronene concentrations ($< 15 \mu\text{g mL}^{-1}$), there was a predominance of HC compounds of DBE = 0-8, comprising *n*-paraffins/isoparaffins (DBE = 0) and cyclic paraffins (cycloalkanes and naphthenes, DBE ≥ 1). When coronene was added at concentrations of 15 and 25 $\mu\text{g mL}^{-1}$, the suppression of cyclic paraffins, compounds with $0 < \text{DBE} < 9$, was first observed, followed by the suppression of *n*-paraffins (DBE = 0), which corresponded to the dominant species. Consequently, the coronene molecule was primarily ionized, giving rise to the peak with DBE = 19.

Saturated fractions analysis

APCI(+)FT-ICR MS was also applied for two saturated fractions (named fractions S_A and S_B , Figures 7a-7b), and the results were compared to GC \times GC/q-MS data (Figure 8). Saturated fractions S_A and S_B , obtained by the SAP method, showed Gaussian profiles of m/z 200-1100 with $M_w = 615$ and 631, respectively (Figures 7a-7b).

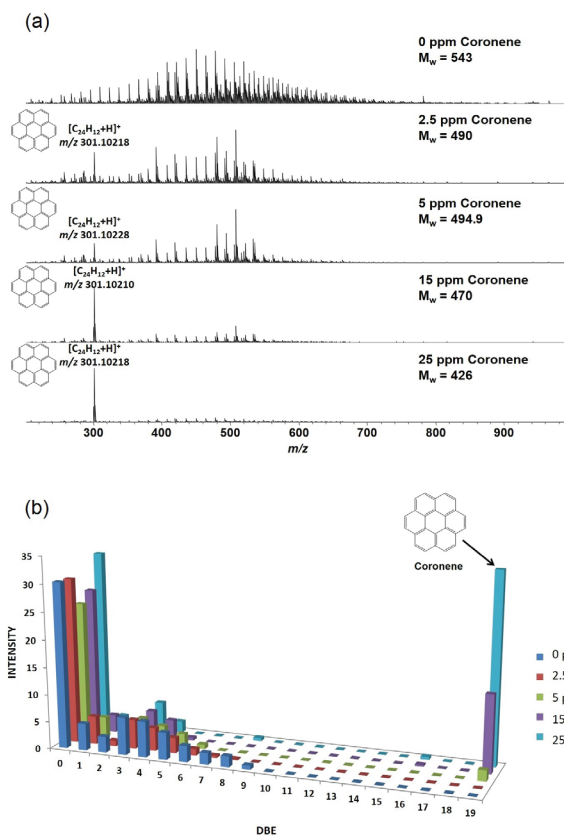


Figure 6. (a) APCI(+)FT-ICR mass spectra of coronene/paraffin blends. (b) DBE distribution for the HC[H] class.

Saturated fractions displayed complex chemical profiles when compared to the data shown in Figure 1. Note a greater predominance of cyclic HC molecules and possibly traces of PAHs containing CNs from C_{15} to C_{78} and DBE 1 to 13 (Figures 7c-7d).

This complex chemical profile was also reflected in the two-dimensional GC data, where detected compounds corresponding to linear HCs; branched HCs; mono-, bi-, tri-, tetra- and penta-cyclic HCs; and PAHs (Figures 8a-8b and Figure S7, SI section). A higher concentration of cyclic paraffin was clearly seen in fraction S_B , as well as the presence of PAHs (in low abundance, Figure 8b). As a consequence, the ionization of *n*-paraffins via APCI(+)MS was affected (Figure 7b). As discussed earlier, PAHs suppressed the ionization of paraffins. On the other hand, for fraction S_A (Figure 7a), *n*-paraffins (CNs of C_{15} - C_{65}) were easily ionized.

Conclusions

Hydrocarbons from non-polar fraction of crude oil can be easily assessed by APCI(+)FT-ICR MS. The distribution of carbon number among paraffin samples were in good agreement with HTGC data. APCI(+)MS was shown to be

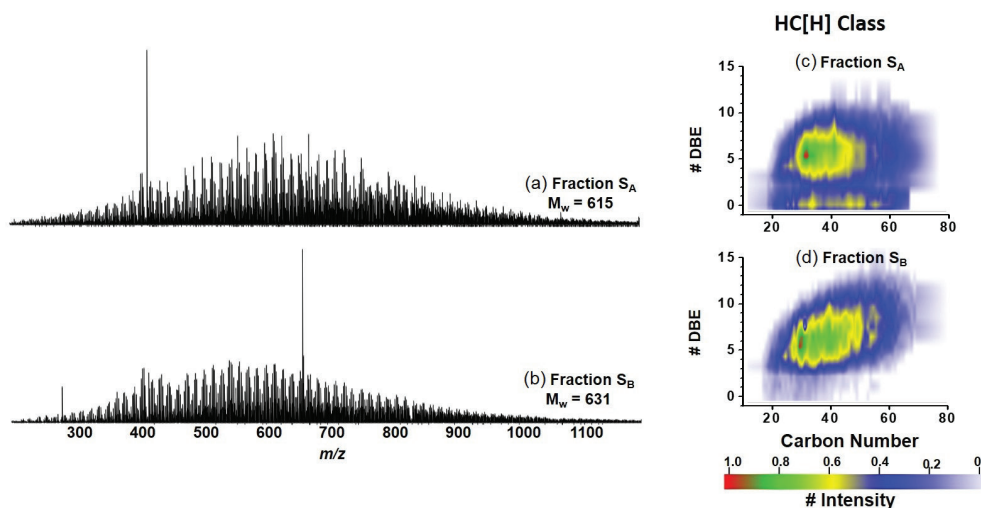


Figure 7. (a, b) APCI(+)-FT-ICR mass spectra of two saturated fractions (S_A and S_B) of Brazilian crude oils and (c, d) their respective DBE versus CN plots.

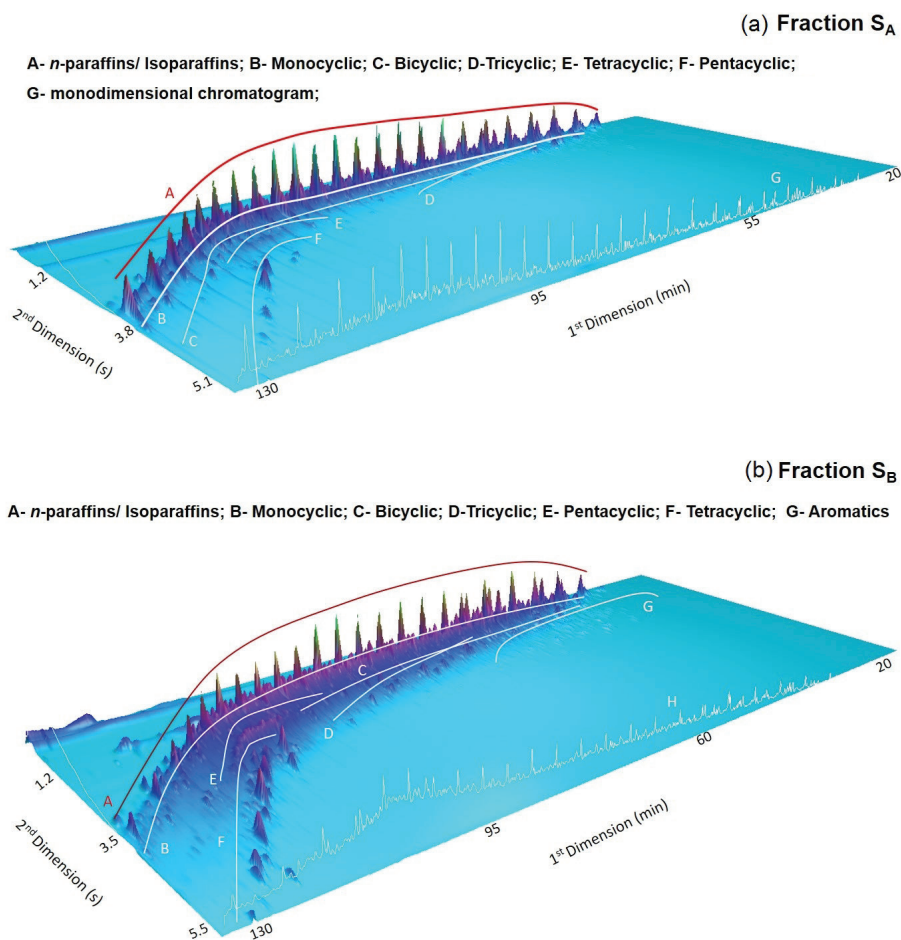


Figure 8. GCxGC/q-MS of the two saturated fractions: (a) S_A and (b) S_B . In both samples, the presence of *n*-paraffins/isoparaffins and cyclic paraffins with DBE = 1-5 (mono, by, tri, tetra and pentacyclic paraffin) was observed. PAHs were detected only in fraction S_B in low abundance.

able to assess paraffin molecules with M_w s of ca. 1200 Da, discriminating carbon numbers from C_{16} to C_{80} .

A good agreement was observed when APCI(+)-MS and ^1H NMR data were compared. The H_β contents

could be directly associated to M_w s that increased in the following order: standard P1 ($M_w = 431$ Da) < standard P2 ($M_w = 444$ Da) < standard P4 ($M_w = 551$ Da) < standard P3 ($M_w = 571$ Da) < standard P5 ($M_w = 662$ Da).

GC×GC/q-MS data from paraffin standards presented good agreement with the DBE *versus* CN plots provided by APCI(+)FT-ICR MS data. Both GC×GC/q-MS and APCI(+)FT-ICR MS indicated the presence of cyclic paraffin in two paraffin standard samples and saturated fractions obtained from SAP method. The presence of PAH at a concentration higher than 25 ppm completely suppressed the ionization of paraffins.

APCI(+)FT-ICR MS using isooctane as reagent gas can be easily used to assess the non-polar information of crude oil samples, so far assessed mostly by electron ionization mass spectrometry or chromatographic techniques. Therefore, as demonstrated here, even in the presence of low proportions of PAHs, paraffin can be ionized using APCI(+)MS.

Supplementary Information

Chromatograms from the HTGC analysis of paraffin standard; chemical profile of CN distribution of paraffin standard; ¹H NMR spectra of paraffin standard; ¹³C NMR spectra of paraffin standard; APCI(+)FT-ICR mass spectra for PAH standards; APCI(+)MS/MS spectra of two PAH standards; and percentage in weight (wt.%) of HCs identified in the two saturated fractions by GC×GC-MS, are available free of charge at <http://jbcs.sbq.org.br> as PDF file.

Acknowledgments

The authors are grateful to CNPq, FAPES and CAPES for financing the research. The authors also thank the Núcleo de Competências em Química do Petróleo (UFES), coordinated by Prof Dr Eustaquio V. R. Castro, for the FT-ICR MS, NMR, HTGC-FID and GC×GC/q-MS analyses as well as to LabPetro for the chemical characterization of the crude oils, and PETROBRAS for providing the crude oil samples.

References

1. Pudenzi, M. A.; Santos, J. M.; Wisniewski Jr., A.; Eberlin, M. N.; *Energy Fuels* **2018**, *32*, 1038.
2. Angolini, C. F.; Pudenzi, M. A.; Batezelli, A.; Eberlin, M. N.; *Encyclopedia of Analytical Chemistry: Applications, Theory and Instrumentation*, 1st ed.; John Wiley & Sons: New York, 2017.
3. Marshall, A. G.; Rodgers, R. P.; *Proc. Natl. Acad. Sci. U. S. A.* **2008**, *105*, 18090.
4. Zhou, X.; Zhang, Y.; Zhao, S.; Chung, K. H.; Xu, C.; Shi, Q.; *Energy Fuels* **2014**, *28*, 417.
5. Zhou, X.; Shi, Q.; Zhang, Y.; Zhao, S.; Zhang, R.; Chung, K. H.; Xu, C.; *Anal. Chem.* **2012**, *84*, 3192.
6. Campbell, J. L.; Crawford, K. E.; Kenttämä, H. I.; *Anal. Chem.* **2004**, *76*, 959.
7. Nyadong, L.; Quinn, J. P.; Hsu, C. S.; Hendrickson, C. L.; Rodgers, R. P.; Marshall, A. G.; *Anal. Chem.* **2012**, *84*, 7131.
8. Vaz, B. G.; Abdelnur, P. V.; Rocha, W. F. C.; Gomes, A. O.; Pereira, R. C. L.; *Energy Fuels* **2013**, *27*, 1873.
9. Klein, G. C.; Kim, S.; Rodgers, R. P.; Marshall, A. G.; Yen, A.; *Energy Fuels* **2006**, *20*, 1973.
10. McKenna, A. M.; Marshall, A. G.; Rodgers, R. P.; *Energy Fuels* **2013**, *27*, 1257.
11. Purcell, J. M.; Merdrignac, I.; Rodgers, R. P.; Marshall, A. G.; Gauthier, T.; Guibard, I.; *Energy Fuels* **2010**, *24*, 2257.
12. Benigni, P.; DeBord, J. D.; Thompson, C.; Gardinali, P.; Fernandez-Lima, F.; *Energy Fuels* **2016**, *30*, 196.
13. Castellanos, A.; Benigni, P.; Hernandez, D. R.; DeBord, J. D.; Ridgeway, M. E.; Park, M. A.; Fernandez-Lima, F.; *Anal. Methods* **2014**, *6*, 9328.
14. Lorente, E.; Berruoco, C.; Herod, A. A.; Millan, M.; Kandiyoti, R.; *Rapid Commun. Mass Spectrom.* **2012**, *26*, 1581.
15. Gao, J.; Owen, B. C.; Borton II, D. J.; Jin, Z.; Kenttämä, H. I.; *J. Am. Soc. Mass Spectrom.* **2012**, *23*, 816.
16. Tose, L. V.; Cardoso, F. M. R.; Fleming, F. P.; Vicente, M. A.; Silva, S. R. C.; Aquije, G. M. F. V.; Vaz, B. G.; Romão, W.; *Fuel* **2015**, *153*, 346.
17. Dias, H. P.; Dixini, P. V.; Almeida, L. C. P.; Vanini, G.; Castro, E. V. R.; Aquije, G. M. F. V.; Gomes, A. O.; Moura, R. R.; Lacerda Jr., V.; Vaz, B. G.; Romão, W.; *Fuel* **2015**, *139*, 328.
18. Freitas, S.; Malacarne, M. M.; Romão, W.; Dalmaschio, G. P.; Castro, E. V. R.; Celante V. G.; Freitas, M. B. J. G.; *Fuel* **2013**, *104*, 656.
19. Hourani, N.; Muller, H.; Adam, F. M.; Panda, S. K.; Witt, M.; Al-Hajji, A. A.; Sarathy, S. M.; *Energy Fuels* **2015**, *29*, 2962.
20. Smit, E.; Rüger, C. P.; Sklorz, M.; De Goede, S.; Zimmermann, R.; Rohwer, E. R.; *Energy Fuels* **2015**, *29*, 5554.
21. Cho, Y.; Witt, M.; Kim, Y. H.; Kim, S.; *Anal. Chem.* **2012**, *84*, 8587.
22. Lydon, C.; DeBord, J. D.; Fernandez-Lima, F.; *Prepr. - Am. Chem. Soc., Div. Energy Fuels* **2013**, *58*, 949.
23. Romão, W.; Tose, L. V.; Vaz, B. G.; Sama, S. G.; Lobinski, R.; Giusti, P.; Carrier, H.; Bouyssiere, B.; *J. Am. Soc. Mass Spectrom.* **2016**, *27*, 182.
24. Adermann, N.; Boggiano, J.; *Composer*, version 1.5.3; Sierra Analytics, Pasadena, CA, USA, 2016.
25. Schmidt, E. M.; Pudenzi, M. A.; Santos, J. M.; Angolini, C. F. F.; Pereira, R. C. L.; Rocha, Y. S.; Denisov, E.; Damoc, E.; Makarov, A.; Eberlin, M. N.; *RSC Adv.* **2018**, *8*, 6183.
26. ASTM D7169-05: *Standard Test Method for Boiling Point Distribution of Samples with Residues such as Crude Oils and*

- Atmospheric and Vacuum Residues by High Temperature Gas Chromatography*; ASTM International: West Conshohocken, Pennsylvania, 2005.
27. Oliveira, E. C. S.; Neto, A. C.; Lacerda Jr., V.; Castro, E. V. R.; de Menezes, S. M. C.; *Fuel* **2014**, *117*, 146.
28. Wu, C.; Qian, K.; Neffiu, M.; Cooks, R. G.; *J. Am. Soc. Mass Spectrom.* **2010**, *21*, 261.
29. Filgueiras, P. R.; Portela, N. A.; Silva, S. R. C.; Castro, E. V. R.; Oliveira, L. M. S. L.; Dias, J. C. M.; Neto, A. C.; Romão, W.; Poppi, R. J.; *Energy Fuels* **2016**, *30*, 1972.
30. Cookson, D. J.; Smith, B. E.; *Anal. Chem.* **1985**, *57*, 864.
31. Speight, R. J.; Rourke, J. P.; Wong, A.; Barrow, N. S.; Ellis, P.; Bishop, P. T.; Smith, M. E.; *Solid State Nucl. Magn. Reson.* **2011**, *39*, 58.
32. Sperber, O.; Kaminsky, W.; Geißler, A.; *Pet. Sci. Technol.* **2005**, *23*, 47.
33. Alcazar-Vara, L. A.; Garcia-Martinez, J. Á.; Buenrostro-Gonzalez, E.; *Fuel* **2012**, *93*, 200.
34. Espada, J. J.; Coutinho, J. A.; Peña, J. L.; *Energy Fuels* **2010**, *21*, 1837.
35. Deursen, Mv.; Beens, J.; Reijenga, J.; Lipman, P.; Cramers, C.; *J. High Resolut. Chromatogr.* **2000**, *23*, 507.
36. Martos, C.; Coto, B.; Espada, J. J.; Robustillo, M. D.; Gómez, S.; Peña, J. L.; *Energy Fuels* **2008**, *22*, 708.
37. Coto, B.; Martos, C.; Espada, J. J.; Robustillo, M. D.; Peña, J. L.; *Fuel* **2010**, *89*, 1087.
38. Welthagen, W.; Schnelle-Kreis, J.; Zimmermann, R.; *J. Chromatogr. A* **2003**, *1019*, 233.

Submitted: August 28, 2018

Published online: December 18, 2018

